

**EPTT-2024-0015**

# **NUMERICAL INVESTIGATION OF NATURAL GAS MIXING THROUGH A CURVED SUPERSONIC SEPARATOR WITH GEOMETRY VARIATION AND CENTRIFUGATION**

**Giovanni Ballario Righini**

**Reinaldo Marcondes Orselli, PhD**

Univesidade Federal do ABC, Centro de Engenharia, Modelagem e Ciências Sociais Aplicadas, Avenida dos Estados, 5001, Santo André, SP, Brazil

giovanni.righini@aluno.ufabc.edu.br

reinaldo.orselli@ufabc.edu.br

**Ricardo Galdino da Silva, PhD**

Instituto de Aeronáutica e Espaço, Departamento de Ciência e Tecnologia Aeroespacial, Praça Marechal Eduardo Gomes, 50, São José dos Campos, SP, Brazil

ri\_galdino@yahoo.com.br

**Denis Fernando Grégorio Junior, BSc**

**Bruno Souza Carmo, PhD**

University of São Paulo, Escola Politécnica, Department of Mechanical Engineering, Av. Prof. Mello Moraes, 2231, São Paulo, SP, Brazil.

denis.fernando@usp.br

bruno.carmo@usp.br

**Abstract.** *The supersonic separator is one of the technologies under development for heavier components separation (especially CO<sub>2</sub>) from natural gas. It is recognized for its efficiency, compact design, and absence of moving parts, which results in reduced maintenance and low footprint. The separation mechanism relies on accelerating the gas to supersonic speed through a convergent-divergent nozzle. In the divergent section, the gas expands, causing a temperature decrease enough to condense the heavier components. Once the heavier components condense, their separation is achieved by imposing a centrifugal force that conducts the droplets toward collectors attached to the nozzle walls. A possible approach to imposing centrifugal force on the flow is to curve the nozzle geometry along the flow path. In order to evaluate the centrifugation effects as well as the curvature on the flow behavior and separation efficiency, the nozzle curvature angle and radius are varied, thereby changing the centrifugal force applied. In this context, CFD simulations with different geometry configurations of the curved nozzle in the supersonic separator are conducted, and the trajectory of the particles is monitored using the Discrete Phase Method (DPM) to assess the impact of centrifugal force on the separation efficiency of the device. The numerical simulations are carried out using the ANSYS Fluent code, which is based on the Finite Volume Method. With the different curvature configurations tested, the centrifugal force attained levels ranging from 111,000 g up to 265,000 g. The maximum separation efficiency observed across these configurations was 71%.*

**Keywords:** *Computacional Fluid Dynamics, Supersonic Separator, Shock Wave, Natural Gas, Fluid Mechanics*

## **1. INTRODUCTION**

The demand for cleaner energy sources is steadily increasing, driven by concerns about the environmental impacts of traditional energy production methods. Transitioning to a cleaner and more sustainable energy system is both a challenge and an opportunity. In this context, new technologies and energy sources need to be developed to meet these demands.

Natural gas emerges as a compelling alternative owing to its lower CO<sub>2</sub> emissions and reduced air pollutants, such as nitrogen and sulfur oxides, compared to coal and oil when utilized for power generation (Silva, 2010). Moreover, natural gas exhibits superior energy efficiency, necessitating less fuel to produce equivalent energy outputs in comparison to coal and oil. This efficiency not only minimizes natural resource consumption but also mitigates environmental impacts

associated with their extraction, transportation, and combustion.

Raw natural gas contains contaminants such as CO<sub>2</sub>, water, and acids, which not only diminish the heating value of the gas but also pose safety hazards and increase transportation expenses due to pipe corrosion (Altam *et al.*, 2017). In response to these challenges, supersonic separators emerge as a promising solution. Their compact size, lack of moving parts and manual operation requirements, and low maintenance make them suitable for offshore installations.

The separation mechanism relies on accelerating the gas to supersonic speed through a convergent-divergent nozzle. As the gas expands in the divergent section, it undergoes a decrease in the static pressure and temperature, leading to the condensation of the heavier components. In order to promote the separation of the condensed components, centrifugation force is imposed to the flow. The liquid droplets formed are conducted by centrifugation towards collectors that are attached on the wall located downstream. The remain natural gas flows downstream up to the nozzle outlet. For axysymmetric flow, a swirler may be used at the subsonic section (Wen *et al.*, 2015; Yang and Wen, 2014; Wen *et al.*, 2010; Wang *et al.*, 2023), however, building and switching different swirlers to vary the centrifugation force can be laborious and complex. Alternatively, the centrifugation may be generated by bending the nozzle at the supersonic section along the streamwise direction, that is, curving the nozzle with a constant radius and arc angle. Although a curved geometry may require a grater footprint, it offers a more flexible and simpler setup, allowing the curvature to be adjusted as needed, especially for experimental tests. Figure 1 illustrates a curved configuration of a supersonic separator developed by Orbital ATK (acquired by Northrop Grumman - [www.northropgrumman.com](http://www.northropgrumman.com)) and ACENT Laboratories (acquired by Calspan - [www.calspan.com](http://www.calspan.com)), depicting the operating principle where the centrifugal force of the curved flow drives the condensed particles towards the collector.

Supersonic separator flows involve high velocity and strong pressure gradients, shock wave formation and reflection, Prandtl-Meyer expansion fans, and interactions of these shock waves with the boundary layer. Careful studies are necessary to investigate these phenomena due to their direct impact on equipment performance. Numerical simulations can be used as valuable tool to investigate the flow behavior in the supersonic separator.

The interaction between the shock wave and the boundary layer may locally promote the shock wave and downstream flow to have a transient or intermittent behavior, however the transient behavior that may occur will not be considered in this work. Numerous studies that address numerical simulations of supersonic separators consider the flow as steady, as reported in Liu *et al.* (2014), Wen *et al.* (2015), Yang and Wen (2014) and Wang *et al.* (2023), among other publications. In fact, the unsteady behavior of the flow occurs locally around the shock wave and the boundary layer, such effects on the overall flow behavior will not be investigated in this work. Despite its higher computation cost, consider the flow as transient can be a topic for a future work so that one may analyze if the flow unsteadiness may cause an impact to the general feature of the flow and separation efficiency.

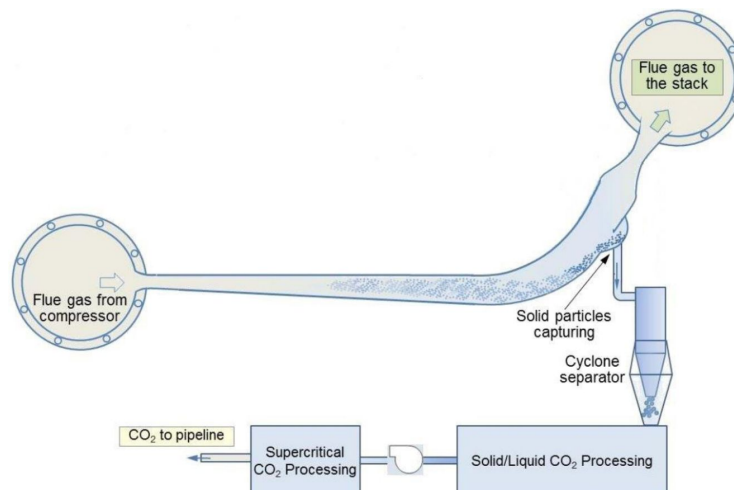


Figure 1: Schematic of ICES process showing the converging-diverging supersonic nozzle for solid CO<sub>2</sub> particle formation, inertial CO<sub>2</sub> capture duct, and pressure recovery in gas diffuser before outlet to the stack (Berger *et al.*, 2017)

## 2. OBJECTIVE

Regarding the scenario mentioned above, the purpose of this work is to perform numerical simulations in order to analyze the influence of the curvature of the curved nozzle of the supersonic separator on the flow behavior and its separation efficiency, as a continuation of the previous work published by Júnior *et al.* (2023) of the same research group as this present work. With the variation of the geometry, data related to different aspects can be obtained, such as the level of centrifugation, velocity distribution inside the device, formation of shock waves and their reflections, and separation

efficiency.

For the numerical simulations, the commercial code Ansys Fluent is used, with the solver based on the finite volume method (Versteeg and Malalasekera, 2007). Regarding the computational domain, the analysis being conducted is two-dimensional (2D). The three-dimensional effects that may occur will not be investigated in this work, notably in the work of Baxmann *et al.* (2020) the 3D effect is studied for a simpler nozzle without curvature (in spite of that it may also be considered for a future investigation).

To analyze the effect of centrifugation on separation efficiency, discrete particles representing CO<sub>2</sub> droplets are injected into the flow. The trajectory of these particles is examined to assess their path towards the collector from the main flow, consequently, to determine the separation efficiency. The methodology of tracking separated particles through the flow is known as Discrete Phase Model (DPM) and is implemented within the Ansys Fluent code. The details of the DPM method will be presented in Section 3.2

### 3. METHODOLOGY

The geometry of the curved supersonic separator was constructed and parameterized using SpaceClaim, Ansys own CAD software, while the discretization of the geometry domain was performed using Ansys Meshing. Finally, for the solver code and post-processor, Ansys Fluent was used, where the momentum, mass, and energy conservation equations are iteratively solved within the computational domain, with all equations being discretized using the finite volume method, as described in Versteeg and Malalasekera (2007); the fluid was considered as a continuum and, the gas as compressible.

In order to solve the discretized equations, the pressure-based solver is used. The algorithm of this solver is set such that each discretized equation is resolved in sequence as segregated (Versteeg and Malalasekera, 2007). The algorithm was originally developed for incompressible flows; however, it has been extended and reformulated to handle a wide range of flow conditions beyond its original intent (Ansys, 2013; Maliska, 2004). Furthermore, for coupling the pressure and velocity fields, the SIMPLE (Semi-Implicit Method for Pressure-Linked Equations) algorithm was utilized (Wen *et al.*, 2015; Yang and Wen, 2014; Wen *et al.*, 2010; Wang *et al.*, 2023). In some cases, when the convergence of the discretized equation was difficult to be reached; alternatively the coupled algorithm may be chosen in place of SIMPLE. In the coupled algorithm, the momentum and pressure-based continuity equations are solved in a simultaneous manner. The coupled method relies on an implicit discretization of the pressure gradients terms in the momentum equations and an implicit discretization of mass flux on the face, to finally achieve a full implicit coupling of the equations (Ansys, 2013) (Kurbatskii and Montanari, 2007). This method presents a higher computational cost per interaction if compared with the SIMPLE method.

Despite the pressure-based method being well-known to be applied for incompressible flows due to its segregated way to solve the discretized balanced equations, it is possible to be used for compressible flows as reported in Maliska (2004). In this case, the variation of the density is considered by incorporating the equation of state within the pressure based algorithm. This pressure based algorithm, applied for compressible flows is able to provide good results as shown in Maliska (2004), and other numerical works, these related to the supersonic separator, that were able to provide reliable results such as Wen *et al.* (2015); Yang and Wen (2014); Wen *et al.* (2010); Wang *et al.* (2023).

For compressible flows, the density-based method can be utilized, as it is recommended by Ansys for handling such cases. The density-based solver handles compressible flows by assembling all equations into a single set of linear equations, solving for unknowns such as density, momentum, and internal energy. The pressure is derived from the equation of state. Although it demands more memory, this solver efficiently discretizes and solves the Navier-Stokes equations simultaneously using an implicit or explicit approach, forming a complete coupled linear system (Versteeg and Malalasekera, 2007).

The pressure-based and density-based solvers handle the continuity, momentum, energy, and species equations differently. The pressure-based solver operates by solving the pressure equation to ensure mass conservation. It offers two algorithms: the segregated (SIMPLE), where equations are solved one after the other, and the coupled, which solves the continuity and momentum equations simultaneously. On the other hand, the density-based solver addresses the continuity equation alongside momentum, energy, and species transport as a single, interconnected set. Although this solver demands more computational resources, especially on larger meshes, it efficiently handles the complexities of compressible flow. The decision to use one solver over the other depends on factors such as the performance trade-offs related to memory usage and solver speed. In contrast, the coupled pressure-based solver solves the continuity and momentum equations simultaneously through implicit discretization of pressure gradients and mass flux (Kurbatskii and Montanari, 2007). For the cases simulated here of the supersonic separator, the authors noticed that this full implicit coupling approach showed to be more efficient. While it is primarily suited for moderate compressibility flows, it balances accuracy and efficiency, making it less resource-intensive and faster in many scenarios. Nevertheless, for the present work, the pressure-based is used due to its lower computational cost observed in simulations and its prior use in published studies (Wen *et al.*, 2015; Yang and Wen, 2014; Wen *et al.*, 2010; Wang *et al.*, 2023). As such, a comparison of the pressure based and density based is shown in Fig. 7.

Moreover, a second-order upwind scheme was adopted for all flow variables for the spatial discretization, and no-slip and adiabatic boundary conditions were assumed for the solid walls. Since the numerical solution of the flow through the supersonic separator was obtained through an iterative method, a convergence criterion was defined as recommended for converged simulation by Ansys (2013): a maximum residual value of at least  $1e-6$  for the energy equation, while for the rest of the transport equations, a maximum residual value of at least  $1e-4$ .

Given that the flow in the supersonic separator exhibits high velocities, the flow is highly turbulent. To deal with the turbulent flow, the RANS (Reynolds Averaged Navier-Stokes) equations approach is used, where the RANS equations are generated from the Reynolds decomposition of the Navier-Stokes equations, characterizing flow parameters in terms of a mean value of flow property and a statistical term of its temporal fluctuation. The application of the time-averaged Navier-Stokes equations results in the emergence of a nonlinear term dependent on the fluctuating properties of the fluid known as the Reynolds stress tensor, which is solved through the Boussinesq hypothesis postulating that Reynolds stresses are proportional to the gradients of the mean velocity. The proportionality coefficient is called turbulent viscosity and is a characteristic of the flow, not the fluid (Versteeg and Malalasekera, 2007).

In the literature, there are numerous turbulence models that propose a correlation between turbulent viscosity and various turbulent flow variables and transport equations. The turbulence models considered for this study are the  $k-\epsilon$  RNG (Yakhot *et al.*, 1992) and the  $k-\omega$  SST (Menter, 1994); both models implemented in the Ansys Fluent code (Ansys, 2013).

The working fluid used was pure methane. Given that the inlet pressure is set at 100 bar at the nozzle inlet, as a typical operation pressure used for the supersonic separator, a real gas model should be used as the gas may behave as supercritical fluid. Among the various real gas state equation models available in the code, the Redlich-Kwong equation (Redlich and Kwong, 1949) was employed, as it has been shown to provide accurate results for the flow regime in supersonic separation, as demonstrated in previous published works of Yang and Wen (2014), Wen *et al.* (2015) and Wang *et al.* (2023). This model not only appropriately addresses the imposed flow conditions but is also effective in predicting the flow properties and the shock wave position, as validated by experimental data (Yang and Wen, 2014).

The effects of condensation on the flow were not accounted for in the numerical simulations, as this work is focused on the centrifugation effects on flow behavior due to curvature, specifically analyzing how effectively inserted condensed particles are directed towards a downstream collector attached to the nozzle wall. In fact, the impact of condensation on the flow can be significant in terms of temperature increase, but the effect on pressure is more subtle. The works of Sun *et al.* (2017), Chen *et al.* (2021), Wen *et al.* (2022), and Chen *et al.* (2023) provide examples where temperature increases by up to 15 degrees due to condensation, while pressure changes are less significant. However, the influence of such temperature changes on particle trajectories under centrifugation may be limited due to the high flow velocity, that is, the time is too short such that it is assumed that elevation of temperature, due to condensation, should not interfere significantly the particle track. Moreover, the effect of re-evaporation of remaining droplets downstream is not considered in this study; instead, it is assumed that re-evaporation occurs upstream of the collector. Therefore, the more complex effects of condensation and its implementation are avoided and not addressed for the present study.

### 3.1 GEOMETRY AND MESH

The convergent-divergent nozzle geometry utilized for the numerical simulations, as depicted in Fig. 3, is primarily based on the design developed by Yang and Wen (2014), and serves as a continuation of the previous work by Júnior *et al.* (2023). As soon as the divergent section ends, the nozzle geometry transitions into a curved section leading up to the diffuser, where the shock wave is formed, gradually decelerating the flow towards the nozzle outlet. This curved section is responsible for directing the particles toward the wall and, subsequently, to the collector. In this study, five curvature angles with a mean radius of 221 mm were analyzed:  $90^\circ$ ,  $120^\circ$ ,  $150^\circ$ ,  $180^\circ$ , and  $210^\circ$ ; and for the last two curvature angles, a mean curvature radius of 150 mm was also studied. An example of these geometries, using the case with a  $150^\circ$  curvature angle and a mean radius of 221 mm, is shown in Fig. 2.

A mesh independence analysis was conducted to determine the appropriate number of cells for the numerical simulations. As shown in Fig. 5, the intermediate meshes did not present significant differences compared to the more refined meshes, and, in order to optimize memory usage without compromising accuracy, the intermediate meshes were used. Due to the velocity gradients formed in the shock wave region and the boundary layer, the mesh was refined in the shock wave and wall regions, as shown, for example, for the  $90^\circ$  curvature angle case in Fig. 4.

The non-dimensional distance of the first cell adjacent to the wall, denoted by  $y^+$ , was used as a domain discretization parameter. The non-dimensional distance from the first cell adjacent to the wall is in the range of 40 to 180 to resolve the flow gradients in the boundary layer region for all the studied geometries. Since  $y^+$  ranges from 31 to 500 in all the cases, a log-law wall function is applied to solve the flow velocity gradients of the boundary layer (Versteeg and Malalasekera, 2007).

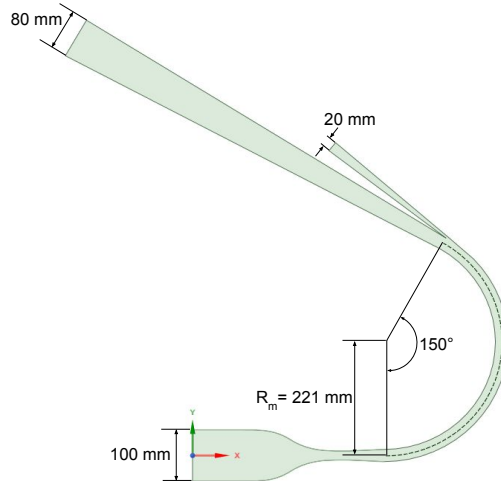


Figure 2: Geometry for the case with a curvature angle of  $150^\circ$  and a mean radius of 221 mm.

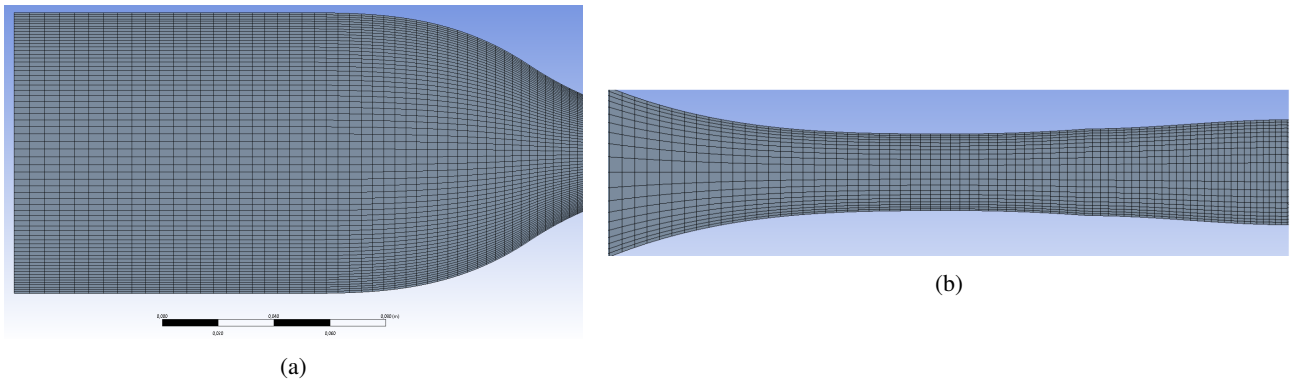


Figure 3: (a) Inlet mesh (b) Converging-diverging section mesh.

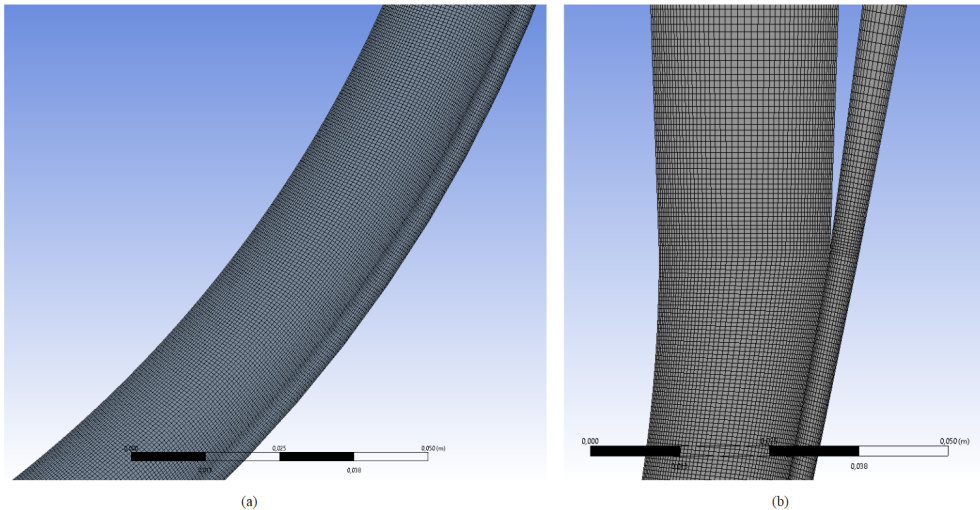


Figure 4: (a) Curved nozzle mesh (b) Diffuser with the gas collector mesh.

### 3.2 Discrete Phase Model

The Discrete Phase Model (DPM) is a multiphase model in which the fluid phase is considered continuous and a second discrete phase is simulated in a Lagrangian reference frame. The discrete phase consists of spherical particles dispersed within the continuous phase, representing particles, droplets, or bubbles. The trajectories of these particles are calculated individually, and they can exchange momentum, mass, and energy with the fluid phase. In this work, the trajectory of the discrete phase was determined considering particle inertia and hydrodynamic drag. Additionally, the displaced fluid volume and particle collisions were neglected, assuming that these effects are insignificant for a discrete

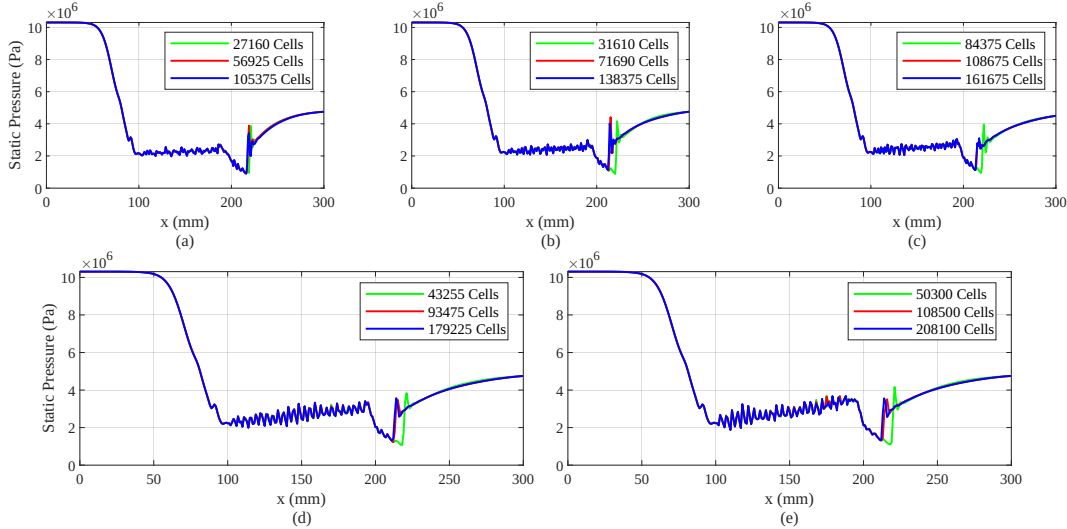


Figure 5: Static pressure values along the center line of the flow for three different mesh refinements with mean curvature radius of 221 mm (a) 90° curvature angle case (b) 120° curvature angle case (c) 150° curvature angle case (d) 180° curvature angle case (e) 210° curvature angle case.

Parameter	Value
Minimum diameter	0.1 $\mu\text{m}$
Maximum diameter	4 $\mu\text{m}$
Mean diameter	1.4 $\mu\text{m}$
Distribution parameter	1.62
Number of diameters	50

Table 1: Parameters of particle diameter distribution for the Rosin-Rammler method.

phase mass flow rate less than 10% of the total fluid flow rate. The particle trajectories were simulated in a steady-state regime, and it was assumed that the fluid phase is not affected by the discrete phase. The particles were injected through a vertical line at the section exactly where the divergent nozzle part ends and the curved nozzle begins. Thus, it is assumed that the condensation with the droplet formation occur as whole at this section position where the temperature and pressure conditions are sufficient to condense  $\text{CO}_2$ . However, the exact location where the droplets are formed is unknown, and difficult to predict; usually is not formed as whole all long the same section (Chen *et al.*, 2023). In fact, the section position where the particles are injected, representing the droplets formation as whole, may be changed and its effect on the separation efficiency may be evaluated, a variation of the position will not be done at this work but it can be investigated for upcoming works. The trajectory of the discrete phase is calculated based on the force balance on each particle, as described in the Lagrangian approach.

To model the droplet size distribution formed during condensation in the supersonic separator, the Rosin-Rammler method (Rosin and Rammler, 1933) available in Fluent was used. Diameters were divided into discrete intervals, and the mass fraction of droplets with a diameter greater than  $d$  is expressed by:

$$Y_d = e^{-(d/\bar{d})^n} \quad (1)$$

where  $\bar{d}$  is the mean diameter and  $n$  is the distribution parameter. The parameters used in this study are listed in Table 1. These were taken from the work of Wen *et al.* (2011), since they have been based by comparison with experimental data.

### 3.2.1 Separation Efficiency

To assess the separation capability of the curved supersonic separator, the separation efficiency for a given particle injection was defined as:

$$\eta = \frac{m_{\text{collected}}}{m_{\text{injected}}} \cdot 100\% \quad (2)$$

where  $m_{\text{collected}}$  is the total mass of all collected particles and  $m_{\text{injected}}$  is the total mass of all injected particles. The particle density was assumed to be constant, with a value equal to the density of  $\text{CO}_2$  in the liquid phase at saturation pressure and 220 K (the average temperature in the curved section of the nozzle across all geometries - see Fig. 8), corresponding to a value of 1160  $\text{kg/m}^3$  (NIST, 2024).

### 3.3 BOUNDARY CONDITIONS

Using the same boundary conditions as in the previous work of Júnior *et al.* (2023), with an increase in inlet pressure, it follows that for all cases analysed, the Mach number at the nozzle inlet is 0.239543, the static inlet pressure is 100 bar, the diffuser outlet pressure is 47.5 bar, and the collector outlet pressure is 45 bar. This configuration ensures that the shock wave occurs downstream the collector inlet, providing the necessary thermodynamic conditions for the condensation of the heavier components, particularly CO<sub>2</sub>. The inlet temperature is 288 K.

## 4. RESULTS

### 4.1 Evaluation of the numerical simulation methodology and setup

The Ansys Fluent CFD code with the pressure-based solver algorithm considering the flow as compressible was tested for a simple convergent-divergent nozzle known as Laval Nozzle as done in previous published work, including Wen *et al.* (2011), Wen *et al.* (2012) and Yang and Wen (2014). The numerical simulation of flow through the nozzle with an Area ratio  $A_{outlet}/A_{throat} = 1.5$  and pressure ratio  $p_{outlet}/p_{inlet} = 0.83049$  was compared with a quasi-one-dimensional Navier Stokes solution developed by Arina (2004). The flow was considered inviscid. The Mach number at the inlet was set to 0.239543. The mesh was build as structured with 1000 volumes in the streamwise direction and 250 volumes in its perpendicular direction.

In Fig. 6, a comparison of the pressure variation along the center line of the nozzle obtained with the present Ansys fluent simulation is compared with the result presented by Arina. It is noticed that both curves agree very well indicating that the current numerical simulation is able to accurately predict the shock wave position as well as able to predict the change of pressure according to the area ratio, and the abrupt change due to the shock wave. Overall, the simulation effectively captures the general behavior of the flow through the supersonic nozzle.

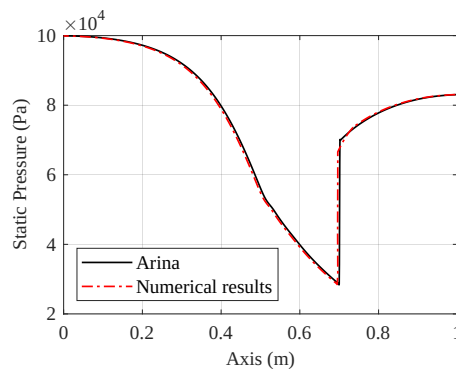


Figure 6: Comparison between the numerical results obtained using the method employed in this work and those obtained by Arina (2004).

The results were also compared using a density-based solver to verify whether the pressure-based solver could accurately predict the flow behavior. Figure 7 shows the results for both solvers, from which it can be seen that there were no significant differences between the two methods, consistent with the discussion on employing the pressure-based solver for this work in Section 3. Since the pressure-based solver is capable of accurately resolving the flow studied in this work and approximately twice as fast as the density-based solver, it was chosen due to its lower computational cost compared

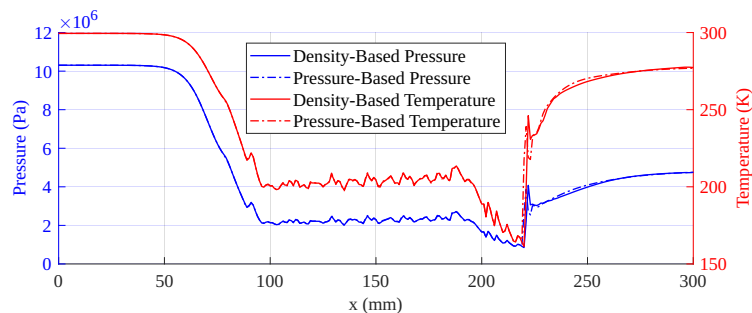


Figure 7: Comparison between the Density-Based and Pressure-Based methods for the case with a 90° curvature angle and a mean radius of 221 mm. For the curves presented, note that for the pressure values refer to the left vertical axis, whereas for the temperature values refer to the values at the right vertical axis.

to the density-based solver.

#### 4.2 Curved nozzle

Given the conditions outlined in Section 3.3, simulations were conducted using both turbulence models (which showed negligible differences) for the geometry configurations. Figure 8 illustrates the results of the Mach number contour field. It can be observed that oblique shocks and Prandtl-Meyer expansion fans are reflected along the curved nozzle in all cases. Immediately after the start of the diffuser and at the collector inlet, a shock wave is present. The interaction between the shock wave and the boundary layer in the diffuser is evident from the flow asymmetry, indicating flow detachment, a phenomenon similarly observed in the study by Haghighi (2010).

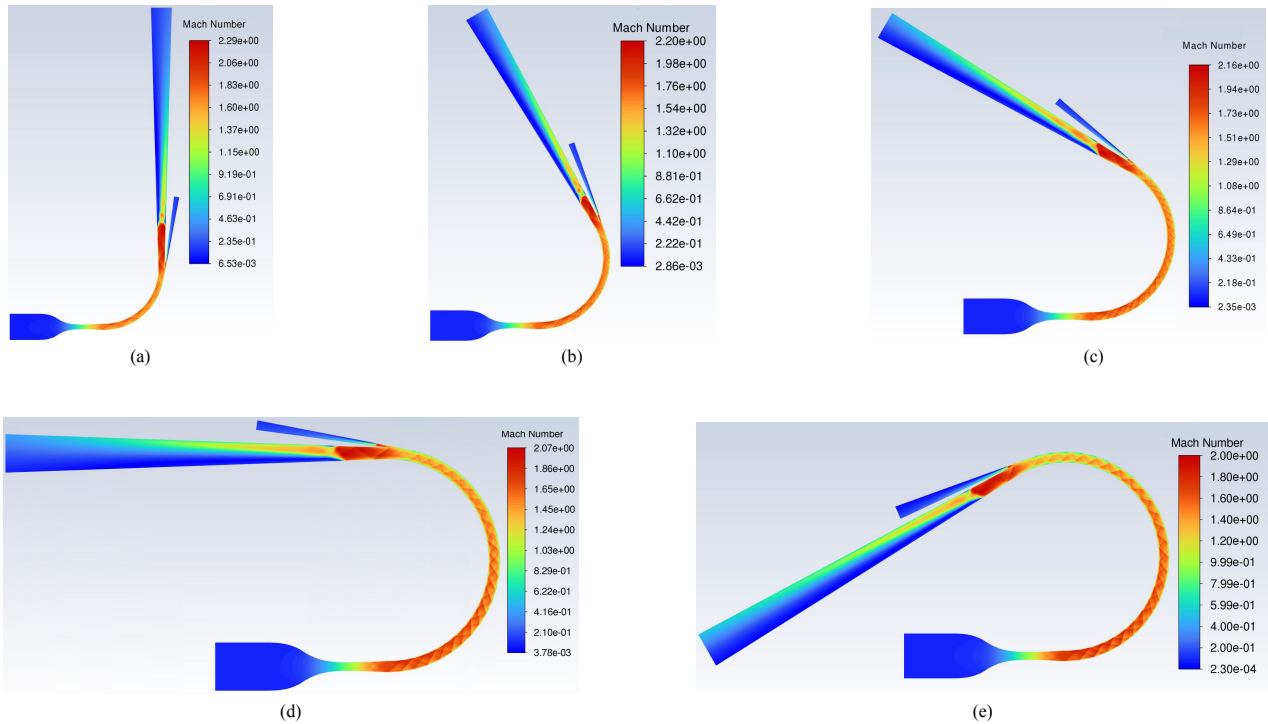


Figure 8: Mach contour field for geometries with mean curvature radius of 221 mm (a) 90° curvature angle case (b) 120° curvature angle case (c) 150° curvature angle case (d) 180° curvature angle case (e) 210° curvature angle case.

A further consideration is that as the curvature of the curved section increases, the Mach number values achieved within the separator decrease. This variation can be attributed to the larger curvature of the nozzle, which results in increased shock reflections and energy dissipation, consequently leading to a lower maximum Mach number. This energy dissipation can also be observed by comparing the static temperature along the centerline of the nozzle, where an increase is noted as the curvature angle becomes larger, as illustrated in Fig. 9.

From Fig. 9, it is observed that the static temperature in the supersonic section of the nozzle reaches values sufficient to condense CO<sub>2</sub> at pressures ranging from 2 to 3.5 bar (as seen in Fig. 5). Therefore, one can conclude that the curved section of the nozzle provides the necessary conditions for the heavier components, primarily CO<sub>2</sub>, to condense (NIST, 2024) and thus be separated from natural gas by the centrifugal force imposed on the flow.

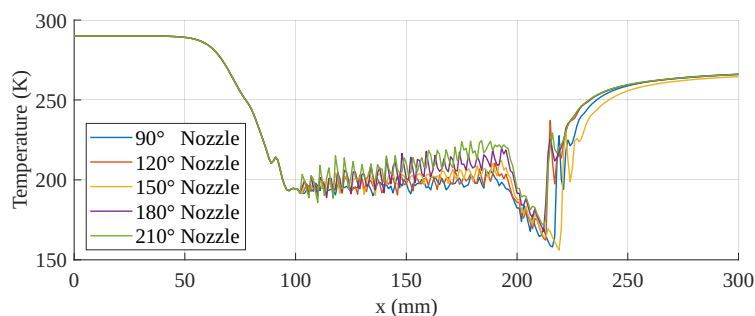


Figure 9: Static temperature along the centerline of the nozzle for different curvature angles.

For all geometries, it is observed that in the curved nozzle, the highest Mach number values are found on the wall with the smaller radius. This is due to the fact that in the region with a smaller radius, the angle between the flow and the curvature induces Prandtl-Meyer expansion waves, thereby increasing the Mach number in that region. In contrast, in the region with a larger radius, oblique shock waves are observed, causing the Mach number to decrease.

The centrifugal acceleration (g-force) experienced by the flow in the curved section of the separator is a central aspect of this study, as it is responsible for directing the condensed particles to the collector. Since the g-force is directly proportional to the tangential velocity of the flow and inversely proportional to the radius of curvature, for cases where the mean radius remains constant, only the velocity affects the g-force. Therefore, as the curved section increases, the g-force experienced by the flow decreases, as seen in Fig. 10.

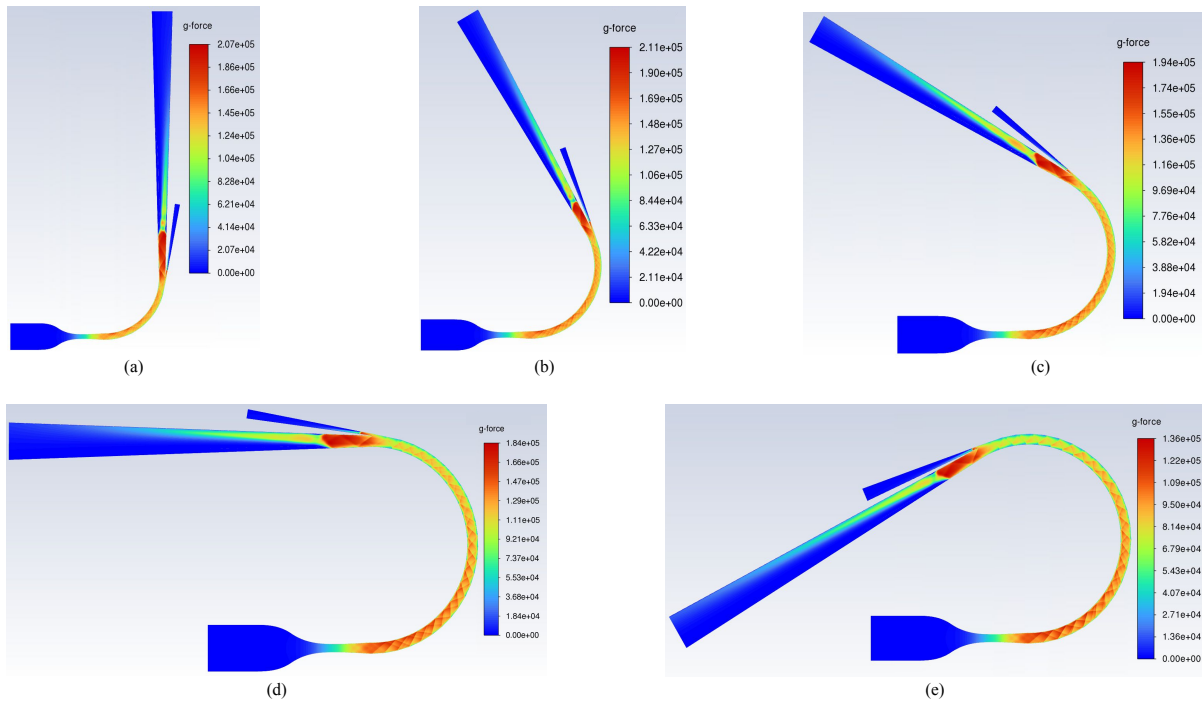


Figure 10: g-force contour field for geometries with mean curvature radius of 221 mm (a) 90° curvature angle case (b) 120° curvature angle case (c) 150° curvature angle case (d) 180° curvature angle case (e) 210° curvature angle case.

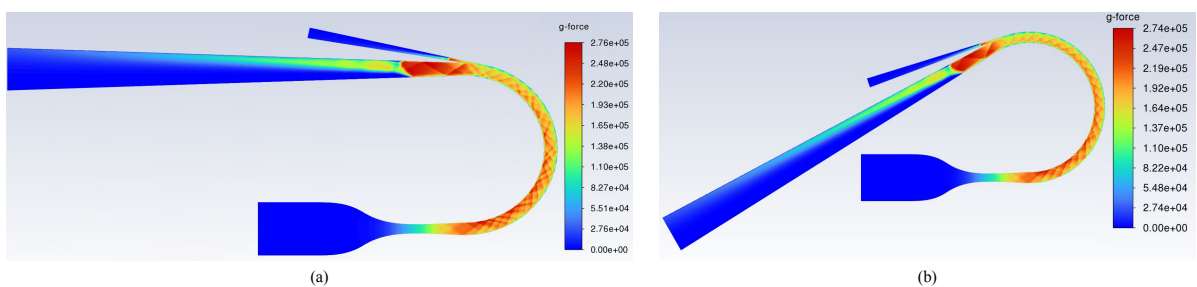


Figure 11: g-force contour field for a mean radius of 150 mm and (a) 180° curvature angle (b) 210° curvature angle.

For cases where the mean radius was altered, a change in the g-force is observed. Figure 11 shows that the maximum g-force values in the curved part of the nozzle are 265000 g and 250000 g for the 180° curvature angle case and the 210° curvature angle case, respectively, both with a mean radius of 150 mm.

Thus, it is evident that for the same mean radius, the maximum centrifugal force is inversely proportional to the curvature angle of the curved nozzle section. This result is better visualized in Fig. 12(a).

### 4.3 DPM simulations

Additional simulations were conducted using the DPM method to evaluate separation efficiency. As expected, the particles are influenced by the centrifugal force generated by the curved section and are directed towards the collector on the outer wall. However, as shown in Fig. 12(b), centrifugal force is not the most decisive factor in separation efficiency. It is observed that, although higher separation efficiency is associated with greater centrifugal force, for the same mean

radius, a higher centrifugal force results in lower efficiency.

It can be seen from Fig. 12(b) and (c) that the highest separation efficiency achieved was approximately 71% for the case with a curvature angle of 210° and an mean radius of 150 mm. This is followed by the case with a 210° curvature and an mean radius of 211 mm, reaching approximately 70% separation efficiency. This suggests the possibility of an optimal ratio between the curvature angle and the mean radius.

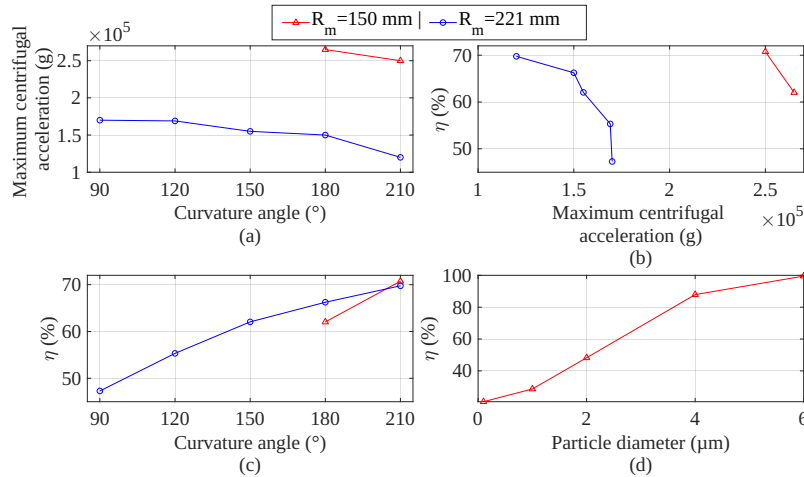


Figure 12: (a) Influence of curvature angle on maximum centrifugal acceleration (b) Relationship between maximum centrifugal acceleration and separation efficiency (c) Relationship between curvature angle and separation efficiency (d) Relationship between particle diameter and separation efficiency.

Figure 12(c) illustrates the influence of the curvature angle on separation efficiency, where it can be observed that for the same mean radius, the greater the curvature angle, the higher the separation efficiency. This is because a larger curvature angle implies a larger curvature arc, providing a greater distance (and time) for the particle to be directed towards the outer wall of the curved section of the nozzle and be collected by the collector. This finding is consistent with the results reported by Wen *et al.* (2012).

The influence of particle diameter on separation efficiency is shown in Fig. 12(d). For a particle diameter set fixed as 0.1  $\mu$ m, the separation efficiency reaches 20%, while for 6  $\mu$ m, it reaches 100%. This is because the density of the CO<sub>2</sub> particles simulated by the DPM method was considered constant; thus, the larger the particle diameter, the greater its mass and the more significant the effect of centrifugal force on it. It is noteworthy that Fig. 12(d) was obtained using the case with the highest achieved efficiency (210° and 150 mm), ensuring that the centrifugal force exerted on the particles was always the same. Subsequently, the diameters of the injected particles were varied, always using the same number of particles. This result is in alignment with the findings obtained by Liu *et al.* (2014) and Duan *et al.* (2019).

## 5. CONCLUSION

In this work, a numerical investigation of the flow behavior in a supersonic separator with a curved nozzle was conducted. The flow domain was considered two-dimensional. The simulations performed show that the nozzle geometries and boundary conditions used are capable of promoting the thermodynamic conditions that lead to the condensation of CO<sub>2</sub>. Additionally, the study aimed to analyze the flow behavior by varying the curvature, as well as to investigate both the effects of curvature and centrifugation on flow behavior and separation efficiency. Furthermore, the relationship between the curvature angle, mean radius of curvature, and the maximum centrifugal acceleration in the flow was analyzed.

By employing DPM simulations, we verified that two geometries achieved the highest separation efficiency: the case with a curvature angle of 210° and a mean radius of 150 mm reached a separation efficiency of approximately 71% for a maximum centrifugal force of 265,000 g; and the case with a curvature angle of 210° and a mean radius of 221 mm achieved approximately 70% separation efficiency for a maximum centrifugal force of 120,000 g. This reinforces the fact that the flow centrifugation significantly impacts separation efficiency, but the relationship between the mean radius and curvature angle is the most decisive parameter for separation efficiency. This suggests that there may be an optimal ratio between these two parameters to achieve higher separation efficiency.

In addition, it was also shown that particle diameter has a significant impact on separation efficiency due to the increased centrifugal force applied to the droplets, demonstrating that, for the conditions analyzed, particles with a fixed diameter of 6  $\mu$ m injected into the throat achieve a separation efficiency of 100% while with 0.1  $\mu$ m reached 20%, however based on experiments, the particle diameters vary as described in section 3.2. Ultimately, since the condensation phenomenon is not considered in the simulations, and a transient analysis was not conducted, these topics may be considered for future work.

## 6. ACKNOWLEDGEMENTS

I would like to thank the RCGI (Research Center for Greenhouse Gas Innovation) hosted by the University of São Paulo (USP) and sponsored by FAPESP – São Paulo Research Foundation; and Shell Brasil for their support and sponsorship of the project. As well as the Federal University of ABC and Coordination for the Improvement of Higher Education Personnel (CAPES) for the financial support in the form of a productivity grant.

## 7. REFERENCES

- Altam, R., Lemma, T. and Juffar, S., 2017. "Trends in supersonic separator design development". *Symposium on Energy Systems*, Vol. 131.
- Ansys, 2013. "Fluent user's guide". <<https://ansyshelp.ansys.com/>>.
- Arina, R., 2004. "Numerical simulation of near-critical fluids". *Applied Numerical Mathematics*, Vol. 51, Issue 4. doi: <https://doi.org/10.1016/j.apnum.2004.06.002>.
- Baxmann, I.L., Orselli, R.M., da Silva, R.G. and Carmo, B.S., 2020. "Numerical simulation assessment for predicting flow through supersonic separator nozzle". In *Proceedings of the 18th Brazilian Congress of Thermal Sciences and Engineering - ENCIT 2020*. Bento Gonçalves, RS, Brazil.
- Berger, A.H., Wang, Y., Bhowan, A.S., Castrogiovanni, A., Kielb, R. and Balepin, V., 2017. "Thermodynamic analysis of post-combustion inertial co2 extraction system". *Energy Procedia*, Vol. 114, pp. 7–16.
- Chen, J., Jiang, W., Han, C. and Liu, Y., 2021. "Numerical study on the influence of supersonic nozzle structure on the swirling condensation characteristics of co2". *Journal of Natural Gas Science and Engineering*, Vol. 88. doi: <https://doi.org/10.1016/j.jngse.2020.103753>.
- Chen, J., Li, A., Huang, Z., Jiang, W. and Xi, G., 2023. "Non-equilibrium condensation in flue gas and migration trajectory of co2 droplets in a supersonic separator". *Energy*, Vol. 276. doi:<https://doi.org/10.1016/j.energy.2023.127589>.
- Duan, Z., Ma, Z., Guo, Y., Zhang, J., Sun, S. and Liang, L., 2019. "Study on supersonic dehydration efficiency of high pressure natural gas". *College to Electromechanical Engineering, Qingdao University of Science and Technology*.
- Haghighi, M., 2010. *Supersonic separators: a gas dehydration device*. Master's thesis, Memorial University of Newfoundland.
- Júnior, D.F.G., Orselli, R.M., da Silva, R.G. and Carmo, B.S., 2023. "Numerical investigation for supersonic gas separator with curved nozzle". In *Proceedings of the 27th International Congress of Mechanical Engineering - COBEM 2023*. Florianópolis, Brazil.
- Kurbatskii, K.A. and Montanari, F., 2007. "Application of pressure-based coupled solver to the problem of hypersonic missiles with aerospikes". In *45th AIAA Aerospace Sciences Meeting and Exhibit*. Reno, Nevada.
- Liu, X., Liu, Z. and Li, Y., 2014. "Investigation on separation efficiency in supersonic separator with gas-droplet flow based on dpm approach". *Separation Science and Technology*, Vol. 49(17), 2603–2612. doi: <https://doi.org/10.1080/01496395.2014.938755>.
- Maliska, C., 2004. *Transferência de calor e mecânica dos fluidos computacional*. LTC, 2nd edition.
- Menter, F., 1994. "Two-equation eddy-viscosity turbulence models for engineering applications". *AIAA Journal*, Vol. 21, pp. 1598–1605.
- NIST, 2024. "Nist chemistry webbook - saturation properties for carbon dioxide". <<https://webbook.nist.gov/chemistry/>>.
- Redlich, O. and Kwong, J.N.S., 1949. "On the thermodynamics of solutions. v. an equation of state. fugacities of gaseous solutions." *Chemical Reviews*, Vol. 44, No. 1, pp. 233–244. doi:10.1021/cr60137a013.
- Rosin, P. and Rammler, E., 1933. "The law governing the fineness of powdered coal". *Journal of the Institute Fuel*, Vol. 7, p. 29–36.
- Silva, I.D., 2010. "Natural gas: its use in electric power generation in brazil". *Magazine for the Petrobras and IF Fluminense university project*, Vol. 1, pp. 103–107.
- Sun, W., Cao, X., Yang, W. and Jin, X., 2017. "Numerical simulation of co2 condensation process from ch4-co2 binary gas mixture in supersonic nozzles". *Separation and Purification Technology*, Vol. 188, Pages 238-249. doi: <https://doi.org/10.1016/j.seppur.2017.07.023>.
- Versteeg, H.K. and Malalasekera, W., 2007. *An introduction to computational fluid dynamics - the finite volume method*. Addison-Wesley-Longman.
- Wang, S., Wang, C., Ding, H., Zhang, Y., Dong, Y. and Wen, C., 2023. "Joule-thomson effect and flow behavior for energy-efficient dehydration of high-pressure natural gas in supersonic separator". *Energy*, Vol. 279. doi: <https://doi.org/10.1016/j.energy.2023.128122>.
- Wen, C., Cao, X., Yang, Y. and Feng, Y., 2015. "Prediction of mass flow rate in supersonic natural gas processing". *Oil Gas Science and Technology*, Vol. 70. 1101-1109. doi:<https://doi.org/10.2516/ogst/201319>.
- Wen, C., Cao, X., Yang, Y. and Li, W., 2011. "An unconventional supersonic liquefied technology for natural gas". *Energy Educ. Sci. Technol.*, Vol. 30, 651-660.
- Wen, C., Cao, X., Yang, Y. and Zhang, J., 2012. "Evaluation of natural gas dehydration in supersonic swirling sep-

- arators applying the discrete particle method”. *Advanced Powder Technology*, Vol. 23, Issue 2, Pages 228-233,. doi:<https://doi.org/10.1016/j.apert.2011.02.012>.
- Wen, C., Cao, X., Zhang, J. and Wu, L., 2010. “Three-dimensional numerical simulation of the supersonic swirling separator”. In *Proceedings of the International Society of Offshore and Polar Engineers*. Beijing, China.
- Wen, C., Li, B., Ding, H., Akrami, M., Zhang, H. and Yang, Y., 2022. “Thermodynamics analysis of co2 condensation in supersonic flows for the potential of clean offshore natural gas processing”. *Applied Energy*, Vol. 310. doi:<https://doi.org/10.1016/j.apenergy.2022.118523>.
- Yakhot, V., Orszag, S., Thangam, S., Gatski, T. and Speziale, C., 1992. “Development of turbulence models for shear flows by a double expansion technique.” *Physics of Fluids A Fluid Dynamics*, Vol. 4.
- Yang, Y. and Wen, C., 2014. “Numerical simulation of real gas flows in natural gas supersonic separation processing”. *Journal of Natural Gas Science and Engineering*.

## 8. RESPONSIBILITY NOTICE

The authors are the only responsible for the printed material included in this paper.